Effect of Negative Poisson's Ratio on the Tensile Properties of Auxetic CFRP Composites

WENHUA LIN and YEQING WANG

ABSTRACT

Carbon fiber reinforced polymer (CFRP) matrix composites have become increasingly popular across industries such as aerospace and automotive industries due to its outstanding mechanical properties and significant weight saving capability. CFRP composites are also widely known to be highly tailorable. For instance, different laminate-level mechanical properties for CFRP composites can be achieved by varying the individual carbon fiber laminar arrangements, among one of them is the Poisson's ratio. Conventional materials have a positive Poisson's ratio (PPR), visualize any conventional materials in a 2D block shape, when stretching that material in longitudinal direction, contraction follows on the transverse direction, whereas for materials with a negative Poisson's ratio (NPR), stretching in the longitudinal direction leads to expansion in the transverse direction. Materials with NPRs have been shown to improve the indentation and impact resistances, when compared to equivalent materials with PPRs. However, producing NPRs could potentially compromise other properties, such as tensile properties, which has not been reported. The current work investigates the effects of NPR on the tensile properties of CFRP composites. Specifically, a laminate-level NPR of -0.4094 in the in-plane direction is achieved through ply arrangement of CFRP composites using classical lamination theory (CLT). The non-auxetic counterpart CFRP composites are designed to produce an PPR of 0.1598 in the in-plane direction while simultaneously match their elastic moduli in three directions with those of the auxetic composites. Results show that the predicted tensile modulus and in-plane Poisson's ratio were in excellent agreement with the experiment results. It was found that the ultimate tensile strength and failure strain or ductility of auxetic specimens were on average 40% lower than those of the conventional CFRP composites.

Wenhua Lin, PhD student, Department of Mechanical & Aerospace Engineering, Syracuse University, Syracuse, NY 13244
Yeqing Wang (corresponding author, email: ywang261@syr.edu), Assistant Professor, Department of Mechanical & Aerospace Engineering, Syracuse University, Syracuse, NY 13244

INTRODUCTION

Carbon fiber reinforced polymer (CFRP) matrix composites have become increasingly popular across industries such as in aerospace, automotive, energy, marine, civil infrastructure, and high-end sports for their high specific mechanical properties and excellent fatigue and corrosion resistances. These properties translate to significant weight savings when compared to conventional metallic materials, such as aluminum. While having superior mechanical performance than conventional metals, CFRP composites are susceptible to various impact damages, such as tool drop impact, hail impact, ballistic impact, and bird strike during their service life. These impacts could lead to various extents of damage modes, such as delamination, matrix cracking, fiber breakage, and penetration, which results in significant degradations in mechanical performances of CFRP [1-4]. One solution to mitigate impact damages, especially low velocity impact damage, for CFRP is to introduce auxeticity or negative Poisson's ratio into the CFRP structure [5-9].

Auxeticity can be introduced into CFRP structures by i) introducing auxetic inclusions or using auxetic matrix and ii) stacking a specific ply arrangement of individual anisotropic lamina. For instance, Li and Wang investigated the effects of auxetic and non-auxetic core materials on the bending behavior of sandwich composites. A negative Poisson's ratio of -1.732 was reported for the sandwich composite with re-entrant honeycomb core [10]. Gunaydin et al. [11] investigated the energy absorption characteristics of chiral auxetic lattices filled cylindrical composite tubes under uniaxial and lateral compression. It was found that the chiral auxetic lattices inserts improved the specific energy absorption by 360% due to the triggered auxetic deformation. Auxeticity can also be produced by stacking a specific ply arrangement of individual anisotropic lamina. A well-validated procedure was proposed by Sun and Li where laminate-level effective moduli, shear moduli, and in-plane and out-of-plane Poisson's ratios can be determined according to the Classical Lamination Theory (CLT) [12]. For instance, researchers have produced laminate-level (or effective) negative Poisson's ratios in the in-plane direction (ν_{12}^{e}) and in the through-thickness direction (ν_{13}^{e}) through tuning the layups of the anisotropic layered carbon fiber reinforced polymer (CFRP) matrix composites [13]. In this study, we focus on auxetic CFRP structures produced by the latter method, i.e., stacking individual anisotropic lamina using a specific layup.

Many studies have reported the enhancement of indentation and impact resistances of auxetic structures, when compared to their non-auxetic counterparts [5-9]. For example, researchers from the University of Bolton (UK) used IM7/5882 carbon fiber reinforced epoxy resin prepregs and produced a negative in-plane Poisson's ratio (i.e., ν_{12}^{e}) of -0.134 with a layup of $[\pm 30]_{6s}$ and a negative through-thickness Poisson's ratio (i.e., ν_{13}^{e}) of -0.156 with a layup of $[0/15/75/15]_{s}$ [14]. Experimental results of quasi-static indentation and low velocity impact tests showed consistently a much smaller damage area (i.e., delamination and fiber breakage) in auxetic composites when compared to non-auxetic composite laminates with matched stiffnesses. Under an impact energy of 18 J, the extent of the damage showed a reduction of 27%.

Despite the many studies conducted to investigate the indentation and impact resistance enhancements for auxetic CFRP composites, effects of negative Poisson's ratio on other mechanical properties, such as tensile strength of CFRP composites are yet to be explored as the imparted negative Poisson's ratios could lead to adverse effects to tensile strength, which is the most advantageous characteristics of CFRP structures. In the current study, we designed CFRP composites with in-plane negative Poisson's ratio and matched non-auxetic counterpart CFRP composites with in-plane positive Poisson's ratio while ensuring close agreement of the three laminate-level effective moduli. Tensile tests were performed to determine the experimentally measured in-plane Poisson's ratio and tensile modulus and evaluate effects of negative Poisson's ratio on the ultimate tensile strength and the failure strain.

LAMINATE-LEVEL EFFECTIVE CONSTANTS

Effective In-Plane Poisson's Ratio

Given the transversely isotropic nature of the individual unidirectional lamina, varying lamina stacking sequence of a CFRP laminate could lead to different laminate-level mechanical properties and the laminate-level in-plane Poisson's ratio is of interest of the current study. The laminate-level in-plane effective Poisson's ratio, ν_{12}^{e}, can be obtained based on the Classical Lamination Theory (CLT),

$$\nu_{12}^{e} = \frac{-J_{21}}{J_{11}} \tag{1}$$

$$\nu_{13}^{e} = \frac{-J_{31}}{J_{11}} \tag{2}$$

where J_{11}, J_{21}, and J_{31} are elements of the **J** matrix,

$$J = A^{-1} + A^{-1}B(D - BA^{-1}B)^{-1}BA^{-1} \tag{3}$$

where **A**, **B**, and **D** are the extensional stiffness matrix, extensional-bending coupling matrix, and bending stiffness matrix according to the CLT. Detailed derivation can be found in author's previous works in [15,16] and Sun and Li [12].

After obtaining the above expressions, a MATLAB code was developed to identify the layup sequences that will produce in-plane negative Poisson's ratio. A final layup sequence consists of five plies of orientation [15/65/15/65/15] was chosen, which produces an in-plane Poisson's ratio of -0.4094.

Effective Moduli

Note that by varying the layup sequence to produce the desired in-plane Poisson's ratio, other mechanical properties are affected at the same time. To effectively investigate the effects of Poisson's ratio on the tensile properties of CFRP composites alone, it is important to minimize effects from other apparent mechanical properties, such as effective moduli in the longitudinal E_1^e, transverse E_2^e and out-of-plane directions E_3^e. The three laminate-level effective moduli can be calculated using the

Table I. Ply-level engineering constants of an IM7/977-3 CFRP composite lamina [17].

Elastic moduli (GPa)	E_{11} = 159, E_{22} = E_{33} = 9.2, G_{12} = G_{13} = 4.37, G_{23} = 2.57
Poisson's ratio	ν_{12} = ν_{13} = 0.253, ν_{23} = 0.456

Table II. Laminate-level effective constants of auxetic and conventional non-auxetic IM7/977-3 CFRP composite laminates.

	Auxetic CFRP composite	**Non-auxetic counterpart CFRP composite**
Layup sequence	[15/65/15/65/15]	[35/60/-5/60/35]
ν_{12}^{e}	-0.4094	0.1598
ν_{13}^{e}	0.6302	0.3629
E_1^e (GPa)	51.2869	51.2935 (+0.0129%)
E_2^e (GPa)	25.5294	21.0296 (-17.626%)
E_3^e (GPa)	9.9504	10.2613 (+3.125%)

well-validated method proposed by Sun and Li, the detailed formulations can be found in Ref. [12]. A MATLAB code was developed to calculate the effective moduli of the specified layup sequence and to identify the layup sequence that could closely match the three effective moduli and at the same time producing a positive Poisson's ratio as counterpart for the auxetic CFRP composite. Table I shows the ply-level engineering constants of the IM7/977-3 carbon fiber composite lamina (i.e., the specific composite considered in this study, see the Materials and Specimens Section) that are used to calculate the effective constants. Table II shows the calculated results of the laminate-level effective constants for both the CFRP composite and the conventional CFRP composite. The layup of the conventional non-auxetic CFRP composite is [35/60/-5/60/35]. In Table II, it can be seen that the longitudinal E_1^e and out-of-plane E_3^e effective moduli could be closely matched with percentage errors of 0.0129% and 3.125%, respectively, whereas the transverse effective modulus had the highest percent error of 17.626%, as it is impossible to match 100% all three effective moduli. Given the primary focus of tensile properties of this study, matching the longitudinal moduli was given the higher priority when selecting the layup sequence.

EXPERIMENTAL SETUP

Materials and Specimens

The CFRP composite specimens used in the current study were manufactured with unidirectional IM7/977-3 carbon fiber prepregs. Following the recommended cure cycle, a 304.8 mm by 304.8 mm CFRP plate was fabricated using the layup orientation of [15/65/15/65/15] for auxetic specimens and [35/60/-5/60/35] for conventional specimens, each having five plies and a final thickness of 0.65 mm. After curing, the fabricated CFRP plates were trimmed to a dimension of 254 mm by 254 mm. Then, a 254 mm by 25.4 mm region was prepared on both front and back surfaces of the CFRP plates and on both top and bottom sides according to ASTM D2093 standard [18] and to be bonded with four 254 mm by 25.4 mm glass fiber tabs using HYSOL EA 9309NA adhesive. The purpose of using the bonded tabs was to avoid damage by the grips during tensile tests given the small thickness of specimens. The CFRP plates with bonded tabs

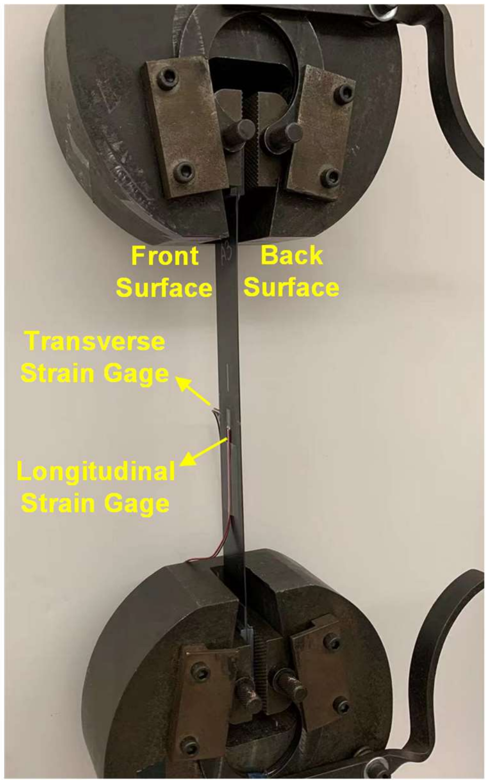

Figure 1. Tensile test grip with loaded specimen prior to testing.

were then cut with a width of 25.4 mm to produce individual specimens which was 254 mm long by 25.4 mm wide and 0.65 mm thick, with four 25.4 mm by 25.4 mm glass fibers tabs on the two ends of both surfaces, making the gage section of the specimens with a dimension of 203.2 mm long by 25.4 mm wide as specified in ASTM D3039 standard [19].

Tensile Test Setup

The tensile tests were carried out according to the ASTM D3039 standard [19] on an MTS testing system with a 100 kN capacity load cell calibrated at 20 kN load, with a self-tightening tensile grip. The tests were displacement controlled with a displacement rate of 1.3 mm/min. To measure the laminate-level Poisson’s ratio, two strain gages were used for each tested specimen, where one strain gage was positioned vertically on the front surface to measure the longitudinal strain and the other was placed horizontally on the back surface to measure the transverse strain, both at the center of the gage section, as shown in Fig. 1.

RESULTS AND DISCUSSION

Tensile Test Results

Figure 2 shows the photograph of all tested specimens, where A denotes the auxetic specimen group and C denotes the counterpart conventional specimen group. It can be seen that both groups have specimen failure towards the end of the gage section instead of at the center and both specimen groups failed predominantly with matrix cracking at the surface plies, at 15° orientation for auxetic specimens and 35° orientation for conventional specimens, along with fiber breakage at embedded plies.

Optical microscopy images of specimens A3 and C3 shown in Figs. 3 and 4 give a better representation of the failure mechanisms. For auxetic specimen A3, clean matrix cracking along the 15° surface plies can be observed. The embedded 65° plies also failed by matrix cracking along with fiber breakage at the exposed edges where the 15° plies failed. Whereas for conventional specimen C3, both the 35° surface plies and embedded plies with 60° and -5° orientation failed with both matrix cracking and fiber breakage. In the microscopy images of the cross section of the tip regions of specimens A3 and C3, delamination between the surface and adjacent plies can be observed in specimen A3. This could be caused by the combined effect of negative Poisson's ratio in the in-plane direction and higher Poisson's ratio in the out-of-plane

Figure 2. Photograph of specimens after tensile tests, where A1-A3 are auxetic CFRP composite specimens (laminate layup: [15/65/15/65/15]) and C1-C3 are non-auxetic counterpart CFRP composite specimens (laminate layup: [35/60/-5/60/35]).

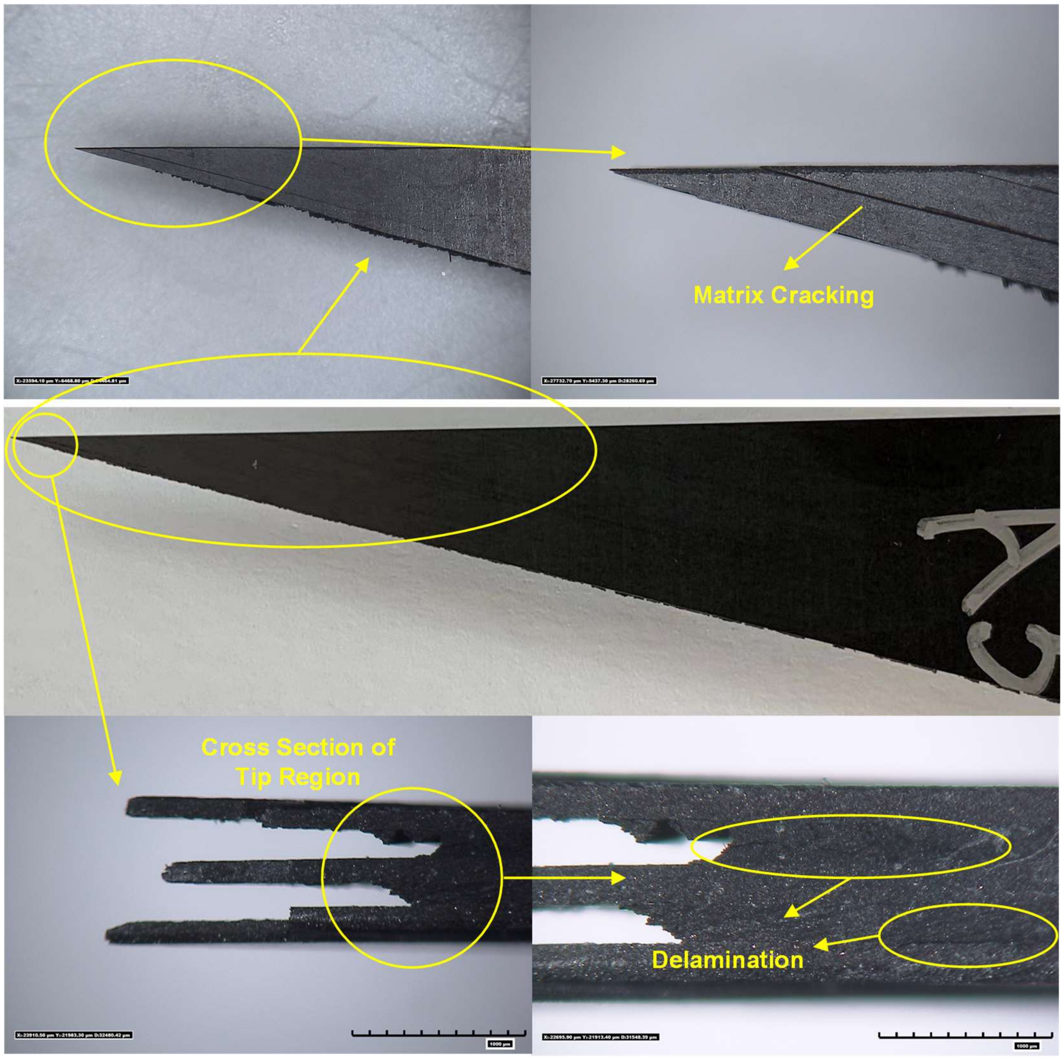

Figure 3. Optical microscopy of auxetic CFRP composite specimen A3 (laminate layup: [15/65/15/65/15], $\nu_{12}^{e} =$ -0.3901, E_1^e=50.92 GPa, see Table III below).

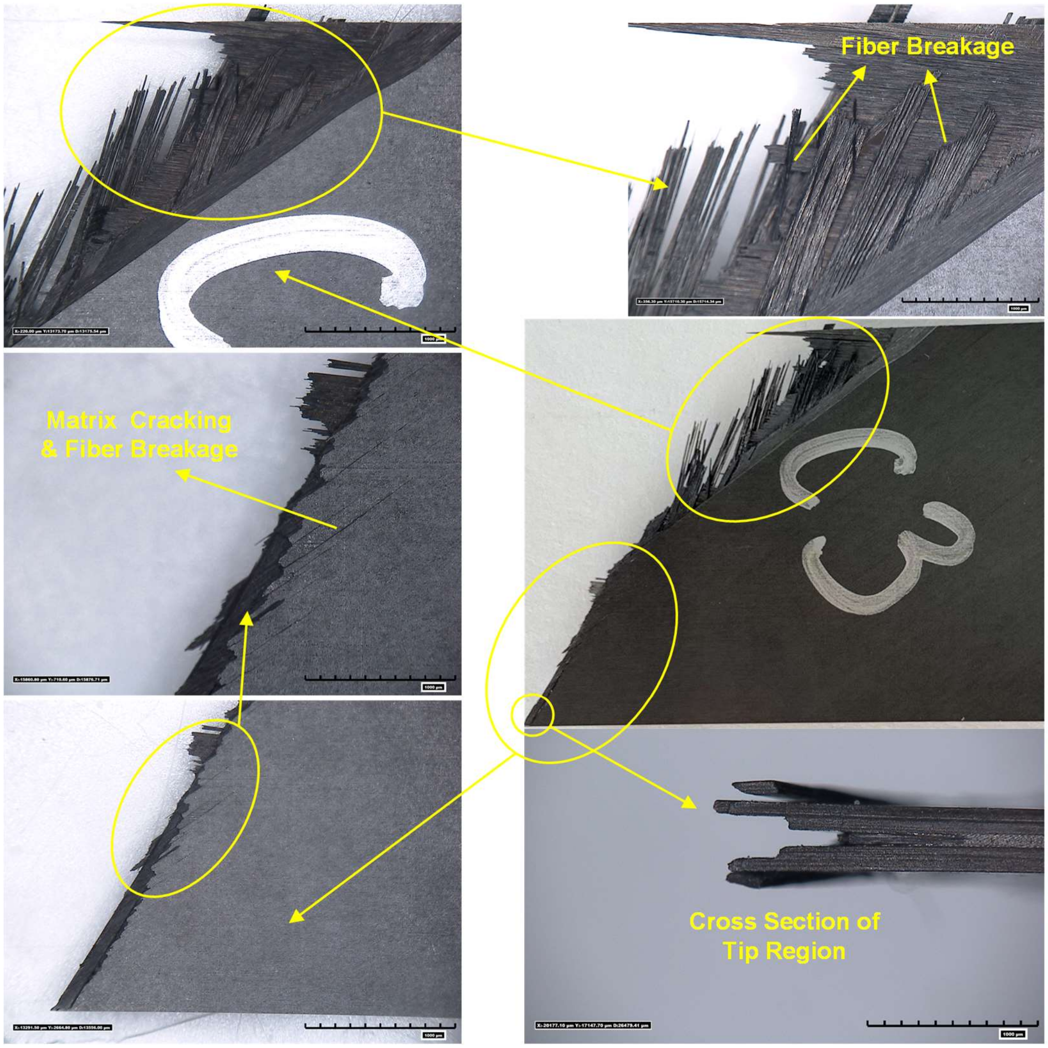

Figure 4. Optical microscopy of conventional non-auxetic counterpart CFRP composite specimen C3 (laminate layup: [35/60/-5/60/35], $\nu_{12}^{e} = 0.1441$, E_1^e=54.44 GPa, see Table III below).

Table III. Experimental and predicted mechanical properties of auxetic (i.e., A1-A3) and non-auxetic (i.e., C1-C3) CFRP composite specimens.

Specimen #	Tensile Modulus Predicted (GPa)	Tensile Modulus Measured (GPa)	Poisson's Ratio Predicted	Poisson's Ratio Measured	Ultimate Tensile Strength Measured (MPa)	Failure Strain Measured (mm/mm)
A1		50.45		-0.4055	323.31	0.00651
A2	51.2869	50.93	-0.4094	-0.4189	317.62	0.00633
A3		50.92		-0.3901	278.31	0.00553
Average	—	50.75 (± 5.67)	—	-0.4048 (± 0.0144)	—	—
C1		54.30		0.1283	558.36	0.01032
C2	51.2935	55.56	0.1598	0.1286	576.02	0.01048
C3		54.44		0.1441	567.72	0.01039
Average	—	54.79 (± 5.43)	—	0.1337 (± 0.009)	—	—

direction of auxetic specimen than conventional specimen. With the layup sequence of [15/65/15/65/15] for auxetic specimen, the in-plane Poisson's ratio (ν_{12}^{e}) is -0.4094 and the out-of-plane Poisson's ratio (ν_{13}^{e}) is 0.6302, in comparison with the in-plane Poisson's ratio (ν_{12}^{e}) of 0.1598 and out-of-plane Poisson's ratio (ν_{13}^{e}) of 0.3629 of conventional specimen with layup sequence of [35/60/-5/60/35]. The combined effect of negative Poisson's ratio in the in-plane direction and higher Poisson's ratio in the out-of-plane direction of auxetic specimen indicates that during tensile loading, the in-plane direction is expanding in both longitudinal and transverse direction while the thickness direction is contracting and could lead to even greater extent of strain mismatch than conventional specimens, thereby causing the delamination.

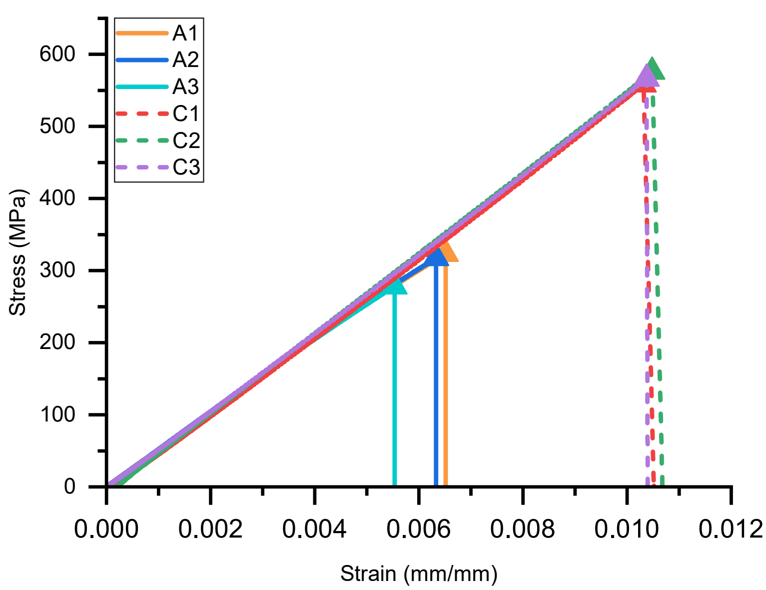

Figure 5. Stress vs. Strain curves for all tested specimens, where A1-A3 are auxetic CFRP composite specimens (laminate layup: [15/65/15/65/15]) and C1-C3 are non-auxetic counterpart CFRP composite specimens (laminate layup: [35/60/-5/60/35]).

Figure 5 shows the stress vs. strain curves for all the tested specimens, it can be observed that all specimens exhibit a brittle failure where the stress vs. strain curves for all specimens increased linearly up to the failure point and immediately dropped to zero beyond the failure point. Table III shows the predicted and experimental mechanical properties data for the auxetic and conventional specimens, the tensile modulus is calculated by finding the slope of the stress vs. strain curves and the Poisson's ratio is calculated by finding the slope between the transverse strain vs. longitudinal strain curves for each specimen. The overall tensile modulus was found to be 50.75 GPa with a standard deviation of 5.67 GPa for auxetic specimens and 54.79 GPa with a standard deviation of 5.43 GPa for conventional specimens. The average in-plane Poisson's ratio was found to be -0.4048 with a standard deviation of 0.0144 for auxetic specimens and 0.1337 with a standard deviation of 0.009 for conventional specimens. Note that the predicted and measured tensile modulus are in excellent agreement where the predicted tensile modulus is 51.2869 GPa for auxetic specimens and 51.2935 GPa for conventional specimens, which have a percent difference of 1.05% and 6.82% from the measured values, respectively.

Even though both layup sequences had similar tensile modulus, the failure strain and ultimate tensile strength of the auxetic specimens on average were only around 60% of those of the conventional specimens, where the average failure strain for conventional specimen was around 1.04%. Note that IM7/977-3 lamina (i.e., a single ply of IM7/977-3, not the laminate) was reported to have a tensile failure strain of 1.61% [20]. The lower ultimate tensile strength and failure strain could also be due to the combined effect of negative Poisson's ratio in the in-plane direction and higher Poisson's ratio in the out-of-plane direction of auxetic specimen where the strain mismatch in the in-plane and out-of-plane directions caused premature delamination and impaired the interface bonding strength between plies causing the lower ultimate tensile strength and failure strain of the auxetic specimens.

CONCLUSION

Auxetic structures were shown to improve the indentation and impact resistances in existing studies. However, producing auxeticity could potentially compromise other properties, such as the tensile properties. The current study investigated the effect of in-plane negative Poisson's ratio on the tensile properties of CFRP composites by designing layup sequence that would produce in-plane negative Poisson's ratio ($\nu_{12}^{e} =$ -0.4094) and then matching counterpart conventional laminates with in-plane positive Poisson's ratio ($\nu_{12}^{e} = 0.1598$) while matching the three laminate-level effective moduli between the auxetic and conventional laminates. Tensile tests were conducted to evaluate the tensile performance of auxetic and conventional non-auxetic specimens followed by photography and optical microscopy to document the failure mechanisms exhibited.

It was found that both auxetic and conventional specimen groups failed in a brittle manner where the stress vs. strain curves increased linearly up to failure point and immediately dropped to zero beyond the yield point. The tensile modulus and the in-plane Poisson's ratio were found to be in excellent agreement with the predicted values. However, the ultimate tensile strength and failure strain or ductility of the auxetic specimens were found to be 40% on average lower than those of the conventional specimens which could be attributed to the combined effect of negative Poisson's ratio in the in-plane direction and higher Poisson's ratio in the out-of-plane direction of auxetic specimen where the greater strain mismatch in the in-plane and out-of-plane directions led to premature failure.

This study suggests that considerations need to be given when designing CFRP structures with negative Poisson's ratio by weighing the desired properties of improved impact resistance and lowered tensile strength. In the future work, we will continue by obtaining the delamination and impact resistances of the two proposed layup sequences. A new auxetic layup sequence will also be investigated which will have good agreement of laminate-level effective moduli with the current layup schedules, but with a lower in-plane negative Poisson's ratio to further investigate the effect of varying the in-plane negative Poisson's ratios on the ultimate tensile strength and ductility of CFRP composites.

REFERENCES

1. Tan W., Falzon B.G., Chiu L.N.S., Price M., Predicting low velocity impact damage and Compression-After-Impact (CAI) behaviour of composite laminates, *Composites Part A: Applied Science and Manufacturing*, 71 (2015) 212-226
2. Lin, W., Wang, Y., Lampkin, S., Philips, W., Prabhakar, S., Smith, R., ... & Rhee, H. (2020). Hail impact testing of stitched carbon fiber epoxy composite laminates. In *35th Annual American Society for Composites Technical Conference,* ASC 2020 (pp. 731-745). DEStech Publications. http://dx.doi.org/10.12783/asc35/34892.
3. Hill, C. B., Wang, Y., & Zhupanska, O. I., "Impact response of CFRP laminates with CNT buckypaper layers," *54th AIAA/ASME/ASCE/AHS/ASC Structures, Structural Dynamics & Materials Conference*, Boston, MA, 2013. http://dx.doi.org/10.2514/6.2013-1617.
4. Hill, C. B., Wang, Y., & Zhupanska, O. I., "Effects of carbon nanotube buckypaper layers on the electrical and impact response of IM7/977-3 composite laminates", *American Society for Composites 27th Annual Technical Conference*, Arlington TX, 2012
5. Li, T., Liu, F., & Wang, L. (2020). Enhancing indentation and impact resistance in auxetic composite materials. *Composites Part B: Engineering*, *198*, 108229.
6. Hou, S., Li, T., Jia, Z., & Wang, L. (2018). Mechanical properties of sandwich composites with 3d-printed auxetic and non-auxetic lattice cores under low velocity impact. *Materials & Design*, *160*, 1305-1321.
7. Alderson, K. L., & Coenen, V. L. (2008). The low velocity impact response of auxetic carbon fibre laminates. *physica status solidi (b)*, *245*(3), 489-496.
8. Allen, T., Shepherd, J., Hewage, T. A. M., Senior, T., Foster, L., & Alderson, A. (2015). Low-kinetic energy impact response of auxetic and conventional open-cell polyurethane foams. *physica status solidi (b)*, *252*(7), 1631-1639.
9. Zhou, L., Zeng, J., Jiang, L., & Hu, H. (2018). Low-velocity impact properties of 3D auxetic textile composite. *Journal of materials science*, *53*(5), 3899-3914.
10. Li, T., & Wang, L. (2017). Bending behavior of sandwich composite structures with tunable 3D-printed core materials. *Composite Structures*, *175*, 46-57.
11. Gunaydin, K., Tamer, A., Turkmen, H. S., Sala, G., & Grande, A. M. (2021). Chiral-lattice-filled composite tubes under uniaxial and lateral quasi-static load: experimental studies. *Applied Sciences*, *11*(9), 3735.
12. Sun, C. T., & Li, S. (1988). Three-dimensional effective elastic constants for thick laminates. *Journal of Composite Materials*, *22*(7), 629-639.
13. Alderson K.L., Simkins V.R., Coenen V.L., Davies P.J., Alderson A., Evans K.E., How to make auxetic fibre reinforced composites, *physica status solidi (b)*, 242 (2005) 509-518
14. Coenen V.L., Alderson K.L., Mechanisms of failure in the static indentation resistance of auxetic carbon fibre laminates, *physica status solidi (b)*, 248 (2011) 66-72.

15. Fan, Y., & Wang, Y. (2020). A study on effect of auxeticity on impact resistance of carbon nanotube reinforced composite laminates. In *Proceedings of the American Society for Composites—Thirty-fifth Technical Conference*. http://dx.doi.org/10.12783/asc35/34959.
16. Fan, Y., & Wang, Y. (2021). The effect of negative Poisson's ratio on the low-velocity impact response of an auxetic nanocomposite laminate beam. *International Journal of Mechanics and Materials in Design*, *17*(1), 153-169.
17. Mohammadi B, Rohanifar M, Salimi-Majd D, Farrokhabadi A. Micromechanical prediction of damage due to transverse ply cracking under fatigue loading in composite laminates. *Journal of Reinforced Plastics and Composites*. 2017;36:377-95.
18. ASTM D2093-03 (2017). Standard Practice for Preparation of Surfaces of Plastics Prior to Adhesive Bonding. *ASTM International*. https://www.astm.org/d2093-03r17.html
19. ASTM D3093 (2017). Standard Test Method for Tensile Properties of Polymer Matrix Composite Materials. *ASTM International. https://www.astm.org/d3039_d3039m-17.html*
20. Clay, S. B., & Knoth, P. M. (2017). Experimental results of quasi-static testing for calibration and validation of composite progressive damage analysis methods. *Journal of Composite Materials*, *51*(10), 1333-1353.